

## Barotropic Models of the Extratropical Response to El Niño

ISAAC M. HELD

*Geophysical Fluid Dynamics Laboratory, Princeton University, Princeton, NJ 08542*

IN-SIK KANG

*Department of Atmospheric Sciences, Seoul National University, Seoul 151 Korea*

(Manuscript received 24 March 1987, in final form 25 June 1987)

### ABSTRACT

A series of linear and nonlinear barotropic models are used to interpret the extratropical response to El Niño equatorial surface temperatures as simulated by an atmospheric general circulation model (GCM). The divergence, time-mean vorticity tendency due to transients, and the zonal mean flow are specified from the GCM, and the deviation of the streamfunction from its zonal mean at an upper-tropospheric level is predicted. Nonlinear steady-state models suggest that the extratropical wave train is primarily forced from the central rather than the western Pacific and that subtropical divergence anomalies are of more importance than tropical anomalies. These nonlinear solutions can be reproduced with little loss in accuracy by linearizing about the zonally asymmetric climatological flow. If one linearizes about the zonally symmetric flow, the part of the solution forced from the western Pacific deteriorates significantly. The solution in the tropics and subtropics also deteriorates if advection of vorticity by the divergent flow is omitted.

Forcing by transients plays a secondary role in generating the extratropical wave train in these barotropic models, but it is pointed out that the subtropical convergence that forces the bulk of this wave train could itself be closely related to anomalies in the transient forcing.

### 1. Introduction

The response in Northern Hemisphere winter to the anomalous tropical latent heating distribution associated with an El Niño–Southern Oscillation event often has the appearance of an equivalent barotropic stationary wave train spanning the North Pacific and North America (Horel and Wallace, 1981). Following Hoskins and Karoly (1981) it is tempting to think of this pattern as an external Rossby wave directly forced by the anomalously large latent heating in the central equatorial Pacific.

The general circulation model experiments of Geisler et al. (1985) suggest that this picture is inadequate. They perform several experiments which differ in the longitudinal position of a tropical sea surface temperature anomaly, yet the longitude of the dominant midlatitude response does not shift appreciably. The positive latent heating anomaly does shift from one experiment to another, as does the upper tropospheric anticyclone pair straddling the equator. The implication is that a model linearized about a zonally symmetric basic state is inadequate for the midlatitude response. Comparing the extratropical responses in two GCMs, Palmer and Mansfield (1986a) support this claim by showing that the response is larger in the model with a more asymmetric climatological extratropical flow. Using a baro-

tropic model, Simmons et al. (1983) stress the importance of the interaction of tropically forced waves with the climatological stationary wave field, and show that this interaction can in some cases be thought of as the excitation of normal modes (either stable or weakly unstable) whose existence is due to zonal asymmetries in the climatological upper tropospheric flow. Frederiksen (1983) finds that these modes exist in baroclinic models as well, and one is led to speculate that such a mode is being excited in the Geisler et al. experiments.

Branstator (1985a) has tested this idea by computing the normal modes of a barotropic model linearized about a GCM's zonally asymmetric upper tropospheric flow, and does not find that a single mode dominates the response. It is conceivable that a fully baroclinic modal decomposition *would* yield one dominant mode; however, Branstator suggests an alternative explanation. He argues that latent heating over the western Pacific and Indian Ocean decreases when positive SST anomalies are introduced into the central or eastern Pacific, regardless of the precise longitude of the anomaly. Branstator goes on to argue that if one linearizes about a zonally asymmetric basic state, then the response over the North Pacific and North America is particularly sensitive to heating in the Indonesian and Indian ocean tropical sectors. The external Rossby wave train could then be understood to first approxi-

mation as the linear response to the decrease in heating in these sectors. Palmer and Mansfield (1986a) also argue for the importance of heating over Indonesia, based on GCM experiments with SST anomalies in the western Pacific, although in their results it is an *increase* in Indonesian heating that produces the same sign of the extratropical anomaly as Geisler et al. find for an increase in central Pacific SST.

In other work of importance for the upper tropospheric response to El Niño, Hendon (1986) and Sardeshmukh and Hoskins (1985) emphasize the importance of nonlinearity for the tropical and subtropical responses. In particular, Hendon shows how nonlinear effects cause the longitude of the subtropical anticyclone pair to shift as the strength of localized tropical forcing is increased. Kok and Opsteegh (1985) go a step further and claim that the extratropical response cannot be understood with any steady-state model, whether it be linear or nonlinear, since the response to the anomalous transient eddy fluxes is of major importance in their linear simulation of the 1982–83 pattern. Palmer and Mansfield (1986b) also suggest that midlatitude transients play a central part in the extratropical response.

We attempt here to gain further insight into the extratropical response to El Niño by mimicking a GCM's behavior as closely as possible with a nonlinear barotropic model. The procedure we follow is identical to that used by Kang and Held (1986) in a study of the climatological upper-tropospheric stationary waves in Northern summer produced by a GCM. The divergence at an upper-tropospheric level and the zonally averaged flow are fixed at the values produced by the GCM; the deviations from zonal symmetry of the streamfunction are then obtained by solving the nonlinear barotropic vorticity equation. The forcing of vorticity by transients produced by the GCM can also be computed and used as an additional forcing for the barotropic model. We find that such a nonlinear barotropic model is able to mimic the GCM's response to El Niño. By removing parts of the forcing and/or linearizing the equation, either about a zonally symmetric or asymmetric flow, we can evaluate the relative importance of central and western Pacific divergence anomalies and forcing by transient vorticity fluxes for the extratropical wave train. This approach has the obvious limitation that it does not explain how the forcing functions in such a barotropic study, the anomalies in the divergence and transient eddy fluxes, are in turn forced by the tropical precipitation anomaly.

## 2. The GCM's response and the barotropic model

Lau (1985) has described the integration of a low-resolution spectral GCM in which sea surface temperatures are set equal to their climatological seasonally varying values everywhere except in the equatorial Pa-

cific, where temperatures are set to those observed during the years 1962–76. The circulation statistics from this calculation have been composited over three El Niño (1965–66, 69–70, 72–73) and three anti-El Niño (64–65, 70–71, 73–74) winters. The difference between the 300 mb streamfunctions, with the zonal mean removed, is shown in Fig. 1a. The corresponding difference in the divergence at the same level is shown in Fig. 1b, while Fig. 1c shows the difference in the precipitation rate. The increase in rainfall in the tropical central Pacific near the dateline is accompanied by upper-tropospheric divergence and a well-defined anticyclone pair straddling the equator. The extratropical wave train that seems to emerge from the Northern Hemispheric anticyclone results in a low over the Gulf of Alaska, a high over northern Canada, and a low on the eastern seaboard of the United States. The similarity of the wave train to that in Horel and Wallace (1981) is encouraging. See Kang and Lau (1986) for further discussion of the extratropical response. (The wave train is also similar to that produced in the perpetual January calculations of Geisler et al., 1985, and Palmer and Mansfield, 1986a, using SST anomalies based on the Rasmussen-Carpenter, 1982, composite.) The drying over Indonesia is smaller in amplitude than the positive central Pacific rainfall anomaly. A large part of the negative rainfall anomaly is located south of the equator, from where one suspects that it will have difficulty in forcing a remote response in the Northern Hemisphere.

Denoting the deviation from the zonal mean by a prime, the equation that we solve on the sphere is

$$\begin{aligned} \partial \zeta' / \partial t &= -\nabla \cdot [(f + \zeta) \mathbf{v}]' + T' - \kappa \zeta' + \nu \nabla^4 \zeta' \\ &= -[\mathbf{v}_\psi \cdot \nabla (f + \zeta)]' - [\mathbf{v}_x \cdot \nabla (f + \zeta)]' \\ &\quad - [(f + \zeta) D]' + T' - \kappa \zeta' + \nu \nabla^4 \zeta', \end{aligned} \quad (1)$$

where  $\mathbf{v}$  is decomposed into rotational and divergent parts,  $\mathbf{v} = \mathbf{v}_\psi + \mathbf{v}_x$ . The time derivative is included only for the purpose of integrating forward until a steady state is reached. The divergence  $D = \nabla \cdot \mathbf{v}_x$  is held fixed at the value predicted by the GCM interpolated to 300 mb, as is the zonally averaged zonal flow. [The GCM's upper-tropospheric divergence in the tropics is typically shared between the model's  $\sigma$ -coordinate levels at 0.34 and 0.205. However, the equivalent barotropic level for external Rossby waves in midlatitudes is generally closer to 400 mb (see Held et al., 1985). The choice of 300 mb is a compromise based on these considerations.] Note that we include the advection of vorticity by the divergent flow, a term that can have a significant effect on the solution (e.g., Kang and Held, 1986; Sardeshmukh and Hoskins, 1987). Consistent with the GCM, we use a spectral model with rhomboidal truncation at wavenumber 15. The biharmonic diffusion coefficient is set equal to the value used in the GCM,  $\nu = 10^{16} \text{ m}^4 \text{ s}^{-1}$ .

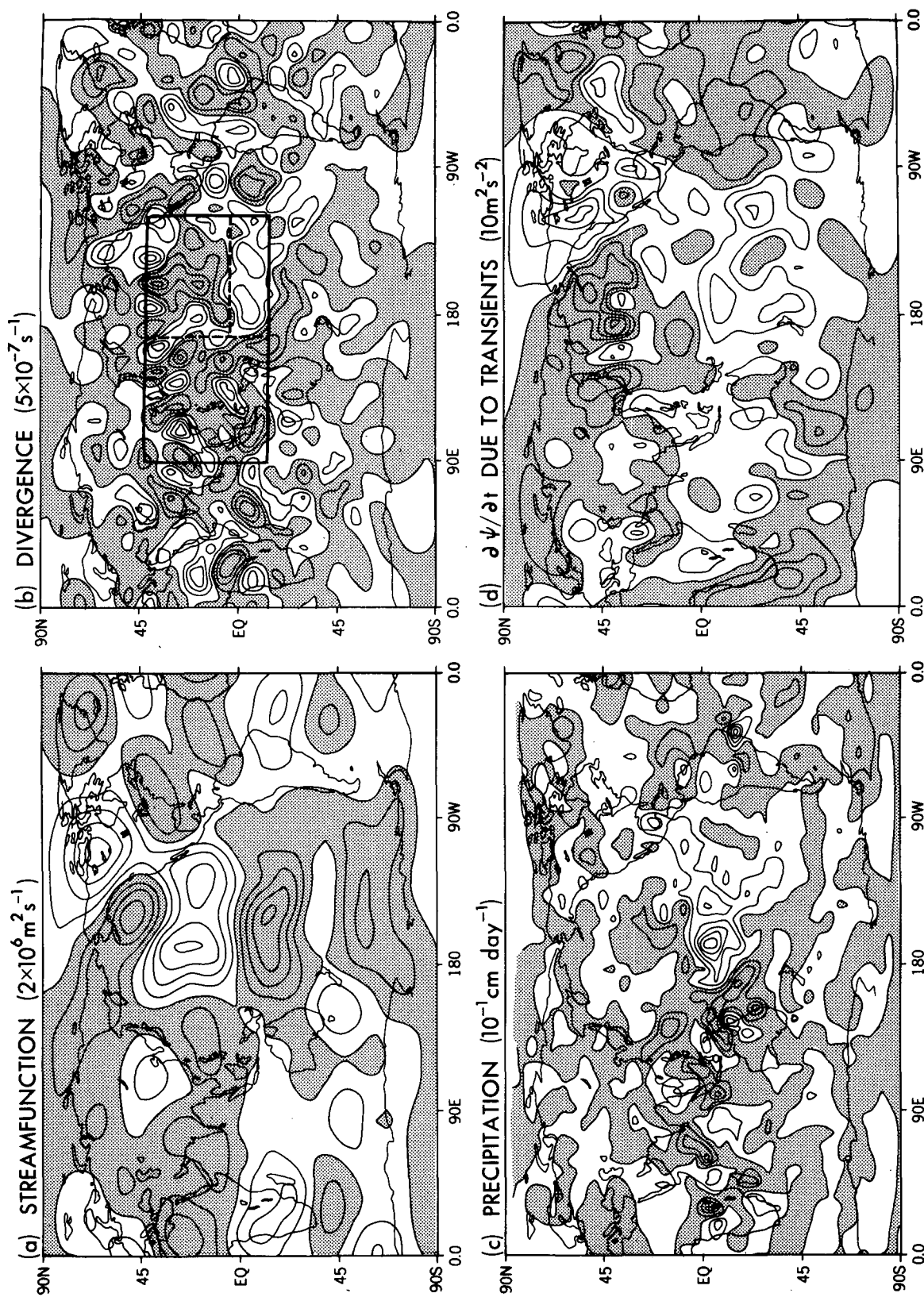


FIG. 1. The difference between the composited El Niño and anti-El Niño (a) 300 mb eddy streamfunction, (b) 300 mb divergence, (c) precipitation rate and (d) 300 mb eddy streamfunction tendency due to transients during Northern winter, from the GCM analyzed by Lau (1985). The solid and dotted rectangles in (b) are referred to in section 3.

The time-mean vorticity tendency due to transients, denoted by  $T$ , is also determined from the GCM. We can compute an approximation to  $T$  by substituting the GCM's mean flow,  $\mathbf{v}_{\text{GCM}}$ , into its full  $\sigma$ -coordinate vorticity equation (including twisting and vertical advection), computing the residual, and then interpolating to 300 mb, ignoring the distinction between the  $\sigma$ -coordinate and  $p$ -coordinate vorticity tendency. More simply, we obtain a good approximation to the transient forcing except on the smallest scales in the model by setting  $T$  equal to  $\nabla \cdot [(f + \zeta_{\text{GCM}})\mathbf{v}_{\text{GCM}}]$  after interpolating  $\mathbf{v}$  to the 300 mb surface. (On small scales, vertical advection and twisting would also contribute to this residual, but there is little point in trying to compute these in pressure coordinates, since they tend to be no larger than the interpolation errors in the dominant terms.) We have used both of these methods. The results obtained differ in some details, but the qualitative behavior of the model and the conclusions we draw from it are unchanged. The results described here are obtained by using the second expression for  $T$ , which is computed for each of the 15 winters. (DJF) of the integration, and then composited in the same way as the flow field. The resulting difference  $\delta T$  between the El Niño and anti-El Niño values of  $T$  is rather noisy; in Fig. 1d we show instead its inverse Laplacian  $\tau = \nabla^{-2}\delta T$ . The small-scale features are sensitive to the method of calculation; some of these are presumably due to vertical advection and twisting rather than true transients. The larger-scale pattern is more robust. There is a strong cyclonic tendency over the North Pacific, and a generally anticyclonic tendency over North America. These streamfunction tendencies are of the same sign as the anomalous streamfunction in these regions.

If the forcing by transients  $T$  is omitted, the barotropic model's simulation of the climatology of the 300 mb streamfunction is severely distorted. Given the possible importance of the climatological stationary waves for the response to anomalous forcing, as demonstrated by Simmons et al. (1983), it is important to retain this term in the calculations. However, we caution the reader that a barotropic model such as this is not an adequate framework for studying the effects of midlatitude transients on the stationary waves. Consider as an example the idealized case in which the only forcing of the stationary eddies is eddy vorticity flux concentrated in a region of very small vertical extent near the tropopause. If we choose to solve our barotropic model at this level, the response to the forcing by transients will be much larger than the true baroclinic response. In a barotropic diagnosis of the sort used in this paper, one would find compensation between the response to the transient forcing and the response to the induced divergence. On the other hand, if the level chosen were below the bulk of the transient forcing, the response to transients would be negligible in the barotropic model, and the entire response would

be forced by the divergence induced by the transients. An additional problem is that the effects of thermal transients will also be felt through the divergence field. One should keep these ambiguities in mind in the following.

The damping  $-\kappa\zeta$  has been included so that steady state solutions are obtained when (1) is integrated forward in time. The choice  $\kappa = 1.5 \times 10^{-6} \text{ s}^{-1}$  is found satisfactory for this purpose, and all of the solutions described in section 3 use this value. The biharmonic diffusion plays a negligible role if  $\kappa$  is large enough to generate a steady state, as it is for the calculations in this paper. The integration procedure is identical to that described in Kang and Held (1986).

### 3. Results

We denote the divergence in the El Niño and anti-El Niño composites as  $D_+$  and  $D_-$  respectively, and set  $D_m = (D_+ + D_-)/2$ , using similar notation for the zonally averaged zonal wind  $U$  and transient forcing  $T$ . Figure 2b shows the solution to (1) with climatological forcing  $D_m$  and  $T_m$  and mean wind  $U_m$ , in a stereographic projection of the Northern Hemisphere. This field should be compared to the GCM's climatological eddy streamfunction shown in the same projection in Fig. 2a. The barotropic solution is somewhat weaker ( $\sim 20\%$ ) because of the Rayleigh friction  $-\kappa\zeta$  needed to ensure a stable steady state, but the basic structure of the stationary eddies is captured rather well. Figure 3b is the difference between two solutions to (1): one with forcing  $D_+$  and  $T_+$  and mean zonal wind  $U_+$ ; and another with  $D_-$ ,  $T_-$ , and  $U_-$ . The agreement with the GCM result (Fig. 3a) is generally good, the most substantial difference in the Pacific-North American sector being the displacement of the anomalous high over Canada to a more southerly location. There are some significant differences in the Atlantic sector, as well.

The composited mean zonal winds,  $U_+$  and  $U_-$ , are very similar to each other, and the solution obtained by setting  $U = U_m$  in both calculations, but varying  $D$  and  $T$ , is sufficiently similar to Fig. 3b that we do not bother to display the result. The shape of the extratropical wave train is unchanged, while the amplitudes of the individual extrema are altered by  $\sim 10\%$ . We set  $U = U_m$  in all of the calculations that follow.

We now choose a domain covering the tropical and subtropical North Pacific, indicated in Fig. 1b by the solid rectangle. This domain contains the largest tropical divergence anomaly as well as the substantial anomaly in the subtropical Pacific. Outside of this domain the divergence and forcing by transients are set equal to their mean values,  $D_m$ ,  $T_m$ ; inside of the rectangle they are set equal to  $D_+$  and  $T_+$  in one calculation and  $D_-$  and  $T_-$  in another. The difference between these two calculations is shown in Fig. 3c, and is seen to be similar to the simulation with the global anomalies in  $D$  and  $T$ , Fig. 3b. The response to the anom-

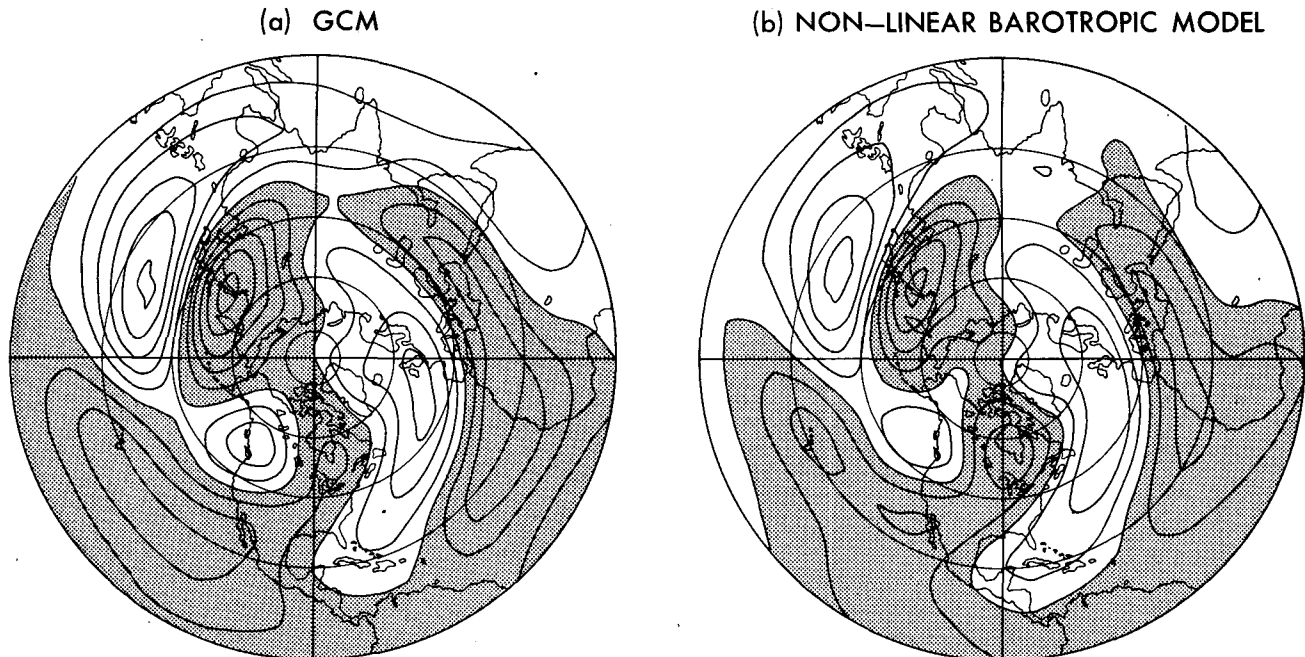


FIG. 2. (a) The GCM's climatological 300 mb streamfunction; (b) the streamfunction produced by the steady barotropic model with damping, using climatological divergence, transient forcing, and zonal mean zonal wind. Contour interval is  $4 \times 10^6 \text{ m}^2 \text{ s}^{-1}$ .

alous  $D$  and  $T$  outside of this rectangle, shown in Fig. 3d, is relatively small over the Pacific and North America, although not entirely negligible. For example, the anomalous high forced by this part of the pattern in the Northeast Pacific pushes the anomalous low in the total simulation northwestward and strengthens the Canadian high anomaly. Despite these differences, the basic character of the extratropical wave train seems to be captured by the forcing within the Pacific rectangle.

We now divide this rectangle into two parts, as shown by the vertical dotted line in Fig. 1b. The western part includes the region of decreased rainfall in the western Pacific; the eastern part covers the large anomalous divergence in the equatorial central Pacific as well as the anomalous convergence in the subtropical central Pacific. Analogous calculations have been performed to those in Figs. 3c, d, but using the forcing  $D$  and  $T$  in one of the smaller rectangles, and using  $D_m$  and  $T_m$  elsewhere. The result for the western Pacific forcing is shown in Fig. 4a and for the central Pacific forcing in 4b.

There is a substantial wave train emanating from the Western Pacific forcing, beginning with a subtropical cyclone at  $140^\circ\text{E}$  and then following an approximate great circle path. The subtropical cyclone is the expected response to the decrease in Indonesian rainfall and is also evident in the total simulation, Fig. 3b. The downstream low in the Gulf of Alaska is nearly as large as the low in the GCM or the full barotropic simulation, but is located  $25^\circ$  to the east. There is little overall

resemblance to the full extratropical response elsewhere.

The response to the central Pacific forcing, on the other hand, bears considerable resemblance to the total response throughout most of the Pacific–North American sector, with the wave train arcing across North America having nearly the correct amplitude and phase. By superposing the patterns forced in the west and central Pacific, one can better understand the pattern resulting from the combined forcing in Fig. 3c. The relatively weak high in 3c over Canada can be seen as due to interference with the large low in the Gulf of Alaska forced from the western Pacific. The center of this low and the center of the low in the North Pacific resulting from central Pacific forcing are separated by  $30^\circ$  of longitude; but there is sufficient constructive interference to produce a low in Fig. 3c that is 25%–30% stronger than that in either Fig. 4a or 4b.

The wave train patterns in Fig. 4a and 4b are similar, but shifted by  $30$ – $40^\circ$  longitude, with the exception of the anticyclone in the eastern subtropical Pacific in Fig. 4b that has no counterpart in Fig. 4a. The response over North America does not appear to be phase-locked by the climatological stationary waves in the manner suggested by Simmons et al. (1983).

The model (1) can be simplified by linearizing about the climatological zonally asymmetric flow, as in Simmons et al. and Branstator (1985a). For a cleaner comparison with the nonlinear models, we actually linearize about the circulation generated in the barotropic model in response to the climatological forcing  $D_m$  and  $T_m$

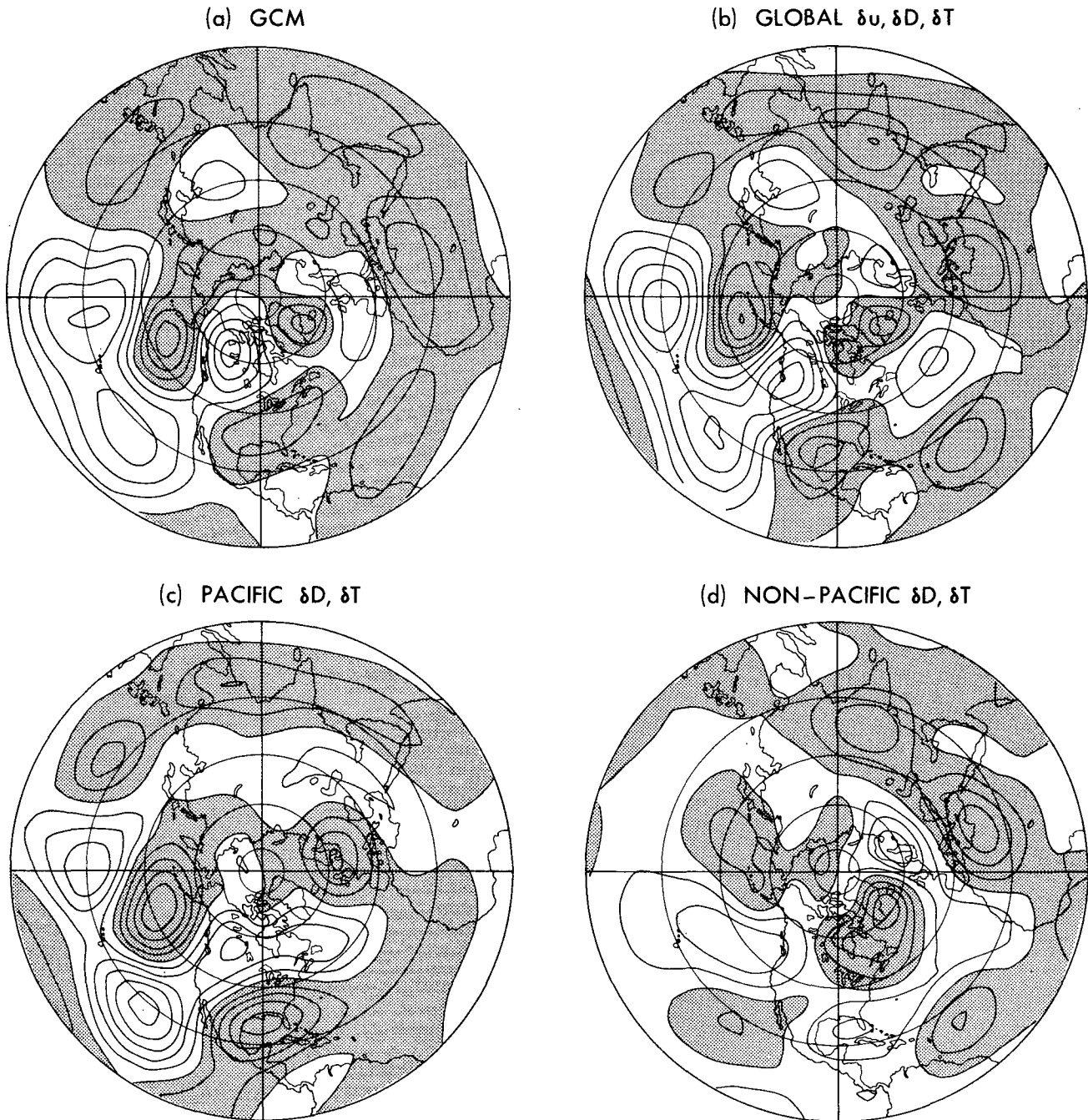


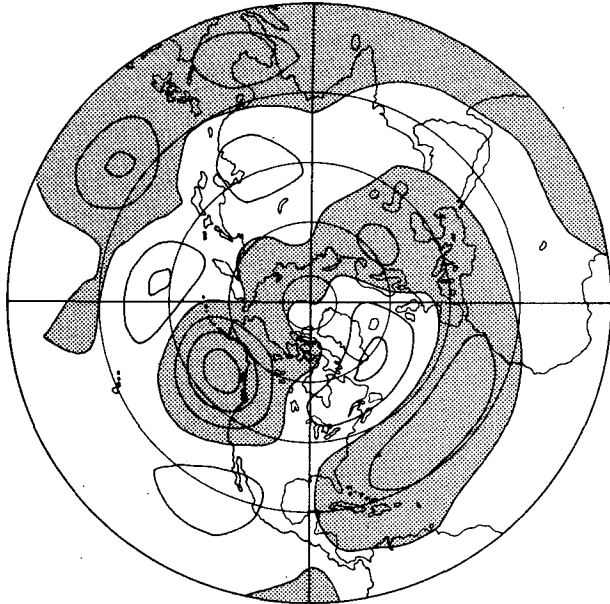
FIG. 3. (a) The composited GCM anomalous eddy streamfunction; (b) the eddy streamfunction produced by the nonlinear barotropic model with anomalous zonal mean wind, and anomalous divergence  $D$  and transient forcing  $T$  over the globe; (c) the prediction with climatological zonal mean wind, climatological  $D$  and  $T$  outside of the Pacific rectangle, and anomalous  $D$  and  $T$  inside the rectangle; (d) the prediction with climatological zonal mean wind, anomalous  $D$  and  $T$  outside of the Pacific rectangle, and climatological  $D$  and  $T$  inside the rectangle. Contour interval is  $2 \times 10^6 \text{ m}^2 \text{ s}^{-1}$ .

(which is very similar to the climatology of the GCM, as illustrated in Fig. 2). Denoting this climatological solution by the subscript  $c$ , we now solve the equation for the anomaly  $\zeta'_a = \zeta'_+ - \zeta'_-$ ,

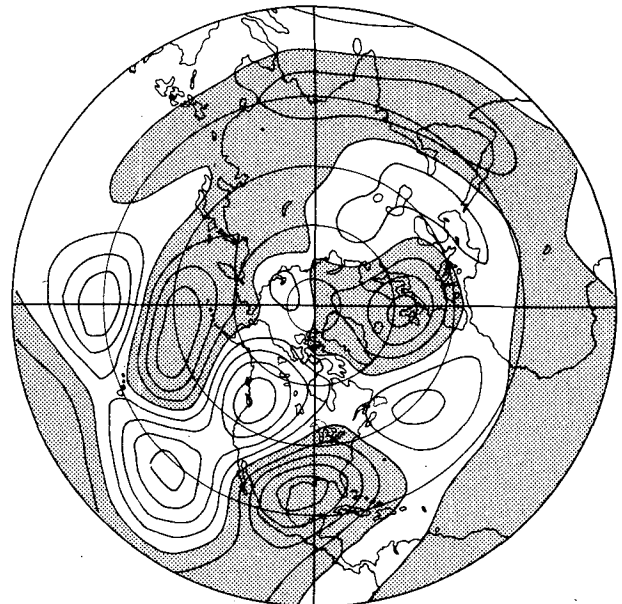
$$0 = -\nabla \cdot [(f + \zeta_c)\mathbf{v}_a]' - \nabla \cdot [(f + \zeta_a)\mathbf{v}_c]' + T'_a - \kappa\zeta'_a + \nu\nabla^4\zeta'_a. \quad (2)$$

The velocity is once again decomposed into rotational

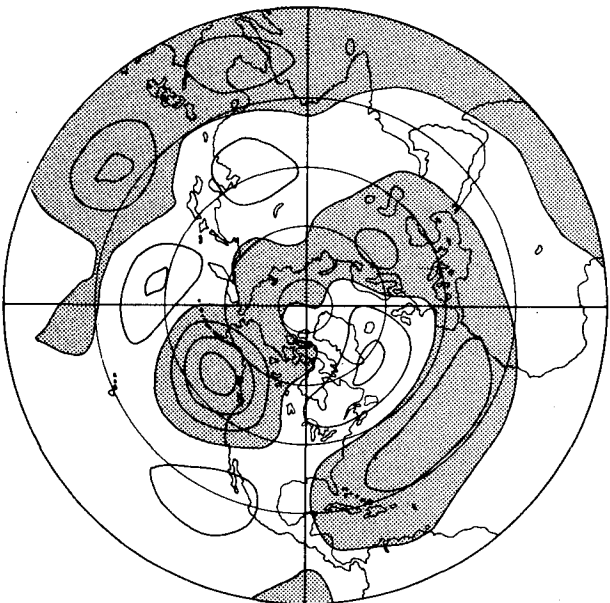
(a) NONLINEAR, WESTERN



(b) NONLINEAR, CENTRAL



(c) LINEAR, WESTERN



(d) LINEAR, CENTRAL

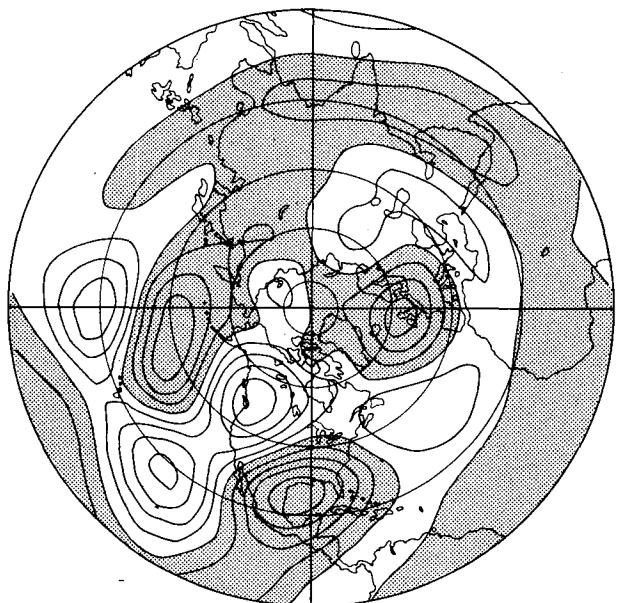


FIG. 4. (a) Streamfunction predicted by the nonlinear model with anomalous  $D$  and  $T$  in the western Pacific and climatological  $D$  and  $T$  elsewhere; (b) as in (a) but for the central Pacific; (c) as in (a) but using a model linearized about the climatological streamfunction; as in (b) but using the linearized model. Contour interval is  $2 \times 10^6 \text{ m}^2 \text{ s}^{-1}$ .

and divergent parts:  $\mathbf{v}_a = \mathbf{v}_{a,\psi} + \mathbf{v}_{a,x}$ ;  $D_a = \nabla \cdot \mathbf{v}_{a,x}$ . The result for the forcing by the divergence  $D_a$  and transience  $T_a$  is shown in Fig. 4c for the western Pacific rectangle and in Fig. 4d for the central Pacific. The results are nearly identical to the fully nonlinear calculations in Fig. 4a and 4b. Therefore, it is justifiable to think of the total response to the anomalous Pacific forcing

as being the linear superposition of its central and western Pacific components, as we implicitly assumed in the preceding discussion. Further experimentation shows that the disagreement between linear and nonlinear solutions increases substantially if one uses  $\zeta_+$  or  $\zeta_-$  for the basic state in (2), rather than  $\zeta_c$ .

(The recent note of E. K. Schneider, 1987, explains

the excellent agreement between the linear and nonlinear models: the difference between the two Jacobians,  $J(\psi_+, \zeta_+) - J(\psi_-, \zeta_-)$ , is equal to  $J(\psi_M, \delta\zeta) + J(\delta\psi, \zeta_M)$ , where  $\delta\psi = \psi_+ - \psi_-$  and  $\psi_M = (\psi_+ + \psi_-)/2$ . From this fact it follows easily that the difference between the two steady solutions to the fully nonlinear problem should be *identical* to that predicted by a model linearized about  $\psi_M$ . The difference between  $\psi_M$  and the solution  $\psi_c$  about which we linearize is very small.)

The central Pacific forcing is subdivided further (by the horizontal dashed line in Fig. 2b) into parts forced by the tropical component of this forcing (south of  $10^\circ\text{N}$ ) which includes the bulk of the positive divergence anomaly, and the remaining subtropical component, which is dominated by a negative divergence anomaly indicative of increased subtropical subsidence. The results shown in Fig. 5a and 5b are obtained with the linear model (2), but the results with the fully nonlinear model are essentially identical. Clearly, the subtropical forcing is predominant. *The upper-tropospheric divergence associated with the tropical precipitation anomaly cannot directly generate the extratropical wave train in a barotropic model.* When one divides the response to the western Pacific forcing in the same way, one finds that it too is dominated by the component north of  $10^\circ\text{N}$ . The small response to the tropical forcing is undoubtedly due to the small values of absolute vorticity  $\zeta_A \equiv f + \zeta$ . As one moves into the subtropics, the forcing  $\zeta_A D$  increases in importance because of the increase in  $\zeta_A$ .

One of the ideas we started out to test was the following: the western Pacific circulation is nearly saturated, in the sense that  $\zeta_A$  is already small; if a portion of the heating moves from western to central Pacific (where  $\zeta_A$  is larger), there will be more anomalous stretching in the central Pacific and that is where the effective Rossby wave source will be. We do find this effect in the responses to tropical divergence; however, these waves forced from the tropics are only a small part of the total response.

In Figs. 2–5 the forcing by transients has been included along with the divergence forcing. The responses to the anomalous divergence in isolation, without the forcing by transients, are shown at the top of Fig. 6, once again using the linear model (2). Comparing with Fig. 4, one finds a substantially weaker response to western Pacific forcing without the transients, with the low off the northwest coast of North America reduced in strength by 30%. The response to central Pacific forcing is also modified; the subtropical high in the eastern Pacific has nearly disappeared, while the high in the subtropical central Pacific has weakened by 40%. With the high in the subtropical east Pacific gone, the wave train now has an orientation more typical of that generated by localized forcing in linear models. This wave train seems to split into two parts over North America, one part progressing across the North Atlantic, and another curving south over the United States. Rossby wave ray tracing on the sphere often leads to such a split (see Figs. 15–17 in Hoskins and Karoly,

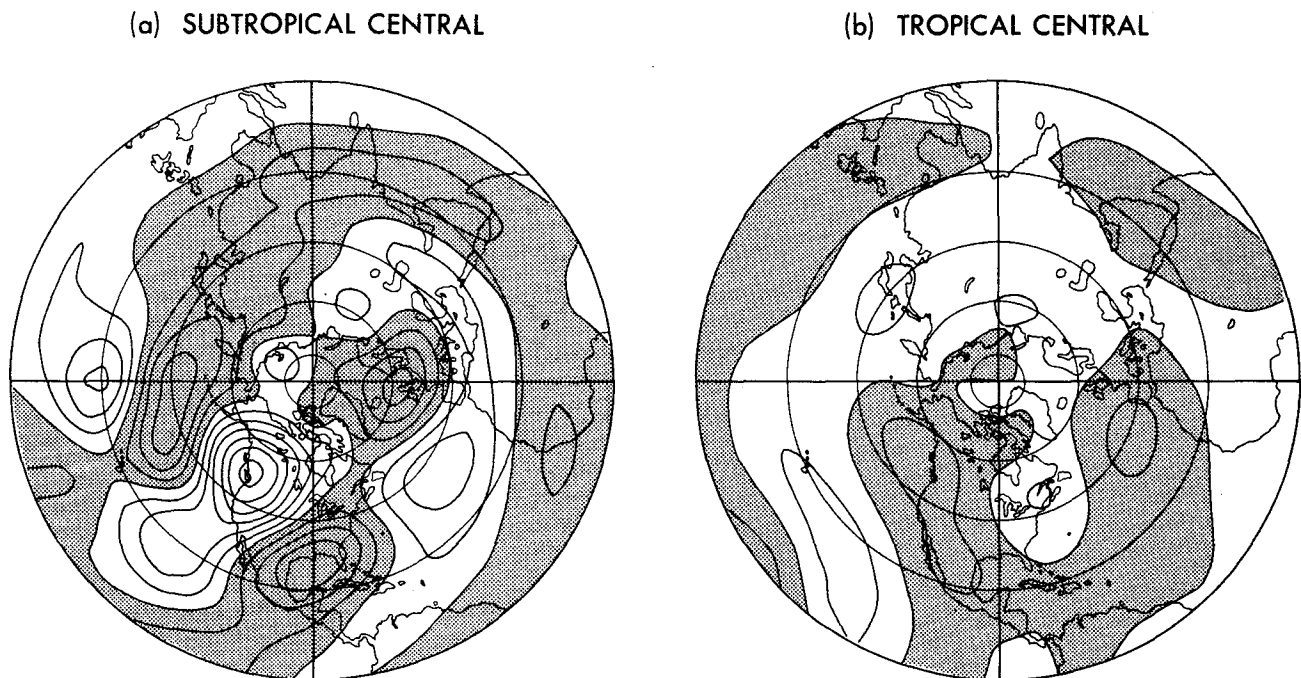
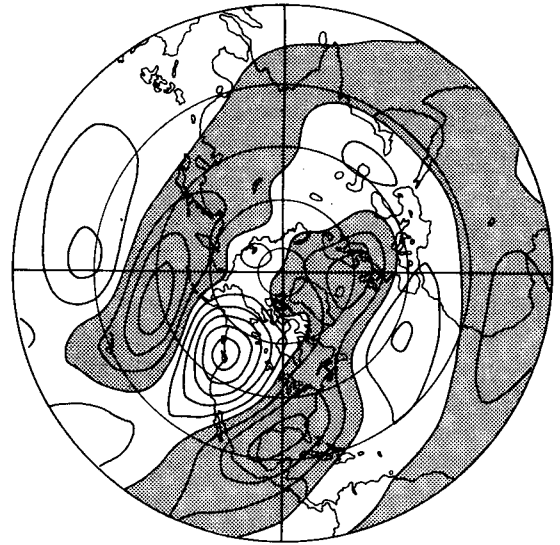
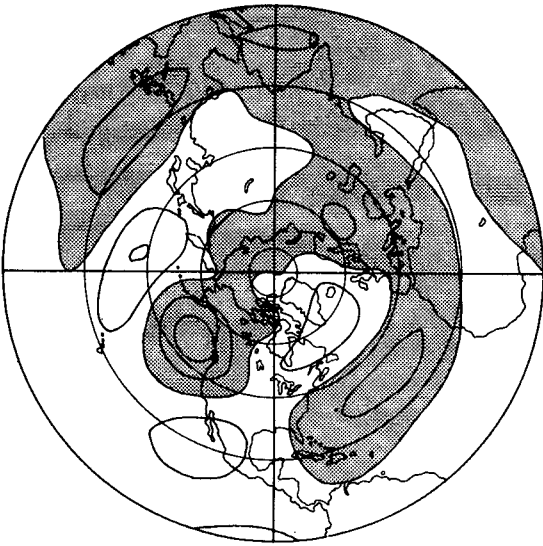


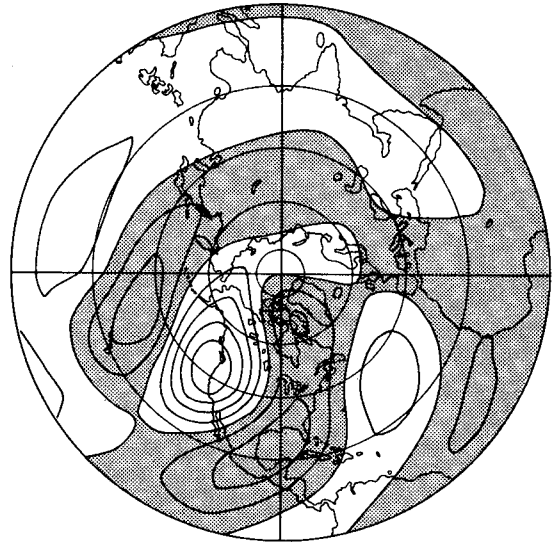
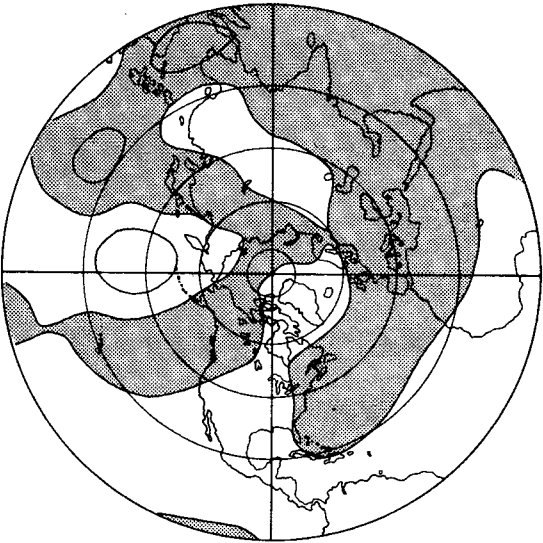
FIG. 5. Streamfunction predicted by model linearized about the climatological streamfunction, for anomalous  $D$  and  $T$  in the (a) subtropical and (b) tropical central Pacific (see Fig. 1b). Contour interval is  $2 \times 10^6 \text{ m}^2 \text{ s}^{-1}$ .



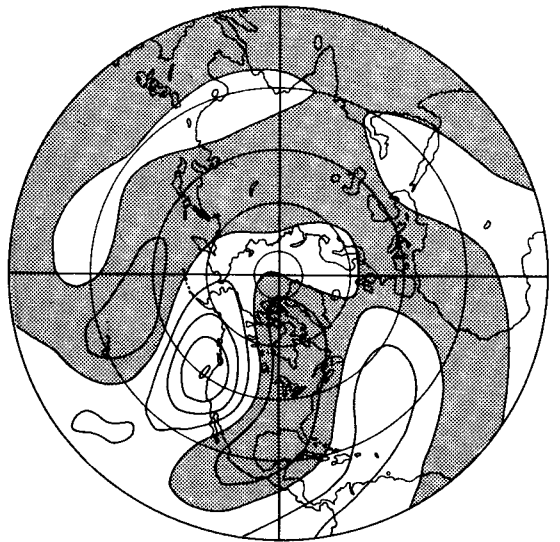
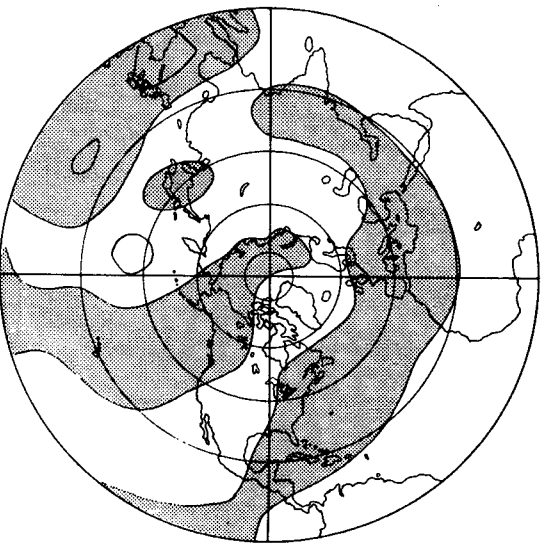
ASYMMETRIC BASIC STATE



SYMMETRIC BASIC STATE



NON-DIVERGENT WITH SYMMETRIC BASIC STATE



WESTERN PACIFIC

CENTRAL PACIFIC

1981). As discussed in section 2, the decomposition of the response into a part forced by the divergence and a part forced by transients can be misleading in such a model, a point we return to in our conclusions.

One can simplify the model further by linearizing about the zonal average of the zonal flow  $U_m$ . The results are displayed in the middle panel of Fig. 6. The response to the western Pacific divergence forcing is most dramatically affected by this simplification, consistent with the results of Simmons et al. (1983). The wave train is displaced equatorward and the low in the Gulf of Alaska is reduced in strength dramatically. The response to the central Pacific divergence is less sensitive to these zonal asymmetries, although the subtropical high in the Pacific is now reduced further, to less than half of its value in the full model (Fig. 4d).

Another simplification is to ignore the advection of vorticity by the divergent component of the flow  $\mathbf{v}_x$ . The possible importance of this term in shifting the effective Rossby wave source poleward has been discussed by Sardeshmukh and Hoskins (1987): when the divergence is embedded in a region of small absolute vorticity, the stretching  $(f + \zeta)D$  is small and the term  $(\mathbf{v}_x \cdot \nabla)\zeta$  can be thought as the dominant source for the extratropical wave train. When this term is dropped in the model linearized about a zonally symmetric flow and forced by the divergence anomaly in the central or western Pacific, the result is as shown in the bottom panels of Fig. 6. While the amplitude of the wave trains is reduced somewhat, the structure of the midlatitude response is not changed dramatically. Since it is not the tropical divergence in regions of small  $f + \zeta$ , but rather the subtropical anomalies where  $f + \zeta$  is large that are important for this response, it is not surprising that the extratropical wave train is not strongly dependent on the  $(\mathbf{v}_x \cdot \nabla)\zeta$  term. However, the tropical response is sensitive to the presence of this term, as in the analysis of the summertime flow by Kang and Held (1986). The subtropical high forced by the central Pacific divergence is hardly present at all when this term (and the effects of transients) are omitted.

#### 4. Conclusions

Barotropic models can be used to help diagnose the GCM's response to tropical SST anomalies. A model linearized about the climatological flow performs as well as a fully nonlinear model, so one can talk of the different parts of the eddy pattern that are forced by different parts of the divergence and transient forcing.

Our barotropic simulations of a GCM response to El Niño boundary conditions do not support the claim that the extratropical wave train in Northern winter

associated with El Niño can be thought of as directly forced by the anomalous upper tropospheric convergence in the tropical western Pacific. While the response to the western Pacific forcing is not negligible, it is generally smaller in the GCM calculation we examine than is the response to forcing in the central Pacific. Furthermore, the results are not suggestive of the preferential excitation of a single linear mode.

The picture is greatly complicated by the fact that it is not the *tropical* divergence in the central Pacific that is the dominant source of the wave train in this barotropic diagnosis. Only in the tropics is there a one-to-one correspondence between vertical motion and precipitation anomalies; so only if the dominant source of the wave train is the tropical divergence can we pretend that the barotropic model is explaining the connection between the *thermal forcing* and the extratropical wave train. In these results, it is the anomalous *subtropical* convergence that is dominant; although it is of the same magnitude as the tropical divergence, it generates larger stretching due to larger values of absolute vorticity. Of course, the subtropical subsidence is itself forced in some way from the tropics. From these barotropic calculations we cannot rule out the possibility that conditions in the western Pacific are of more importance for the subtropical subsidence in the central Pacific than conditions elsewhere in the tropics.

The heating due to this subtropical subsidence is not balanced by a decrease in precipitation. Inspection of the temperature equation shows that it is primarily balanced by anomalous horizontal cold air advection. Since positive correlation between  $v$  and  $w$  is expected in a free external Rossby wave in vertical shear (see Held et al., 1985, p. 871), one must consider the possibility that the divergence anomaly that is the apparent source of the wave train in this model is simply part of a tropically forced Rossby wave.

Alternatively, it is also possible that this subtropical subsidence is itself forced by anomalous transients. The response to the explicit transient forcing in these barotropic simulations is quite large in some regions, as seen in the differences between Fig. 4 and Fig. 6. But given the importance of divergence forcing outside of the tropics, where it is not strongly constrained by the heating field, we cannot rule out the possibility that the anomalous divergence is itself induced by anomalous vorticity transients at other levels (as discussed in section 2). Linear baroclinic calculations to be described elsewhere suggest that this second alternative is indeed relevant—consistent with the results of Kok and Opsteegh (1985) for the El Niño of 1982–83. The picture that emerges is that the response to the tropical heating anomaly, which likely requires nonlinear models to estimate adequately, creates anomalies in

FIG. 6. Streamfunction predicted by various versions of the linear model, as described in text, forced by the central or western Pacific anomalous divergence. Contour interval is  $2 \times 10^6 \text{ m}^2 \text{ s}^{-1}$ .

transient eddy fluxes (and the associated subtropical divergence anomaly) which then exert the primary control over the anomalous extratropical wave pattern.

Given these results, how does one explain the calculations of Geisler et al. wherein the longitude of the extratropical wave train does not shift as the longitude of the SST anomaly is shifted, while the anomalous heating and the tropical response do shift? One possibility is that heating anomalies or the climatological stationary waves are sufficiently different in the two GCMs that the western Pacific forcing is indeed more important in Geisler et al. For example, it is not hard to imagine that a modest northward shift of the rainfall anomaly in the western Pacific could result in a much larger Northern Hemispheric wave train emanating from that region. Alternatively, a full barotropic diagnosis of the Geisler et al. results analogous to that performed here might show the subtropical subsidence in the central Pacific to be the dominant forcing, and the longitude of this subsidence to be insensitive to the longitude of the tropical heating or SST anomaly. This insensitivity could be due either to the direct interaction of the tropically forced waves with the climatological stationary waves or to its interaction with the asymmetric storm tracks.

Calculations with models linearized about a zonally symmetric flow do show considerable differences from those in which the model is linearized about the zonally asymmetric climatological flow, as shown by Fig. 5. This result seems to justify the assertion in Simmons et al. (1983) and Branstator (1985) that it is important to include the interaction between the climatological waves, primarily forced in midlatitudes, and the anomalous tropically forced waves. But it is possible that barotropic calculations overemphasize the importance of this interaction. To illustrate this point, consider a stationary conservative quasi-geostrophic eddy, linearized about a zonally symmetric flow  $\bar{u}$  with potential vorticity gradient  $\bar{q}_y$ . Outside of the region of forcing, the eddy potential vorticity is given by  $q' = -(\bar{q}_y/\bar{u})\psi'$ . As has often been noted, if  $\bar{q}_y/\bar{u}$  is independent of  $y$ , then  $J(\psi', q') = 0$ , and the linear solution is also a solution of the fully nonlinear equation. But if the flow consists of waves with different total horizontal wavenumbers,  $J(\psi', \zeta')$  will not vanish in general. Thus, it is possible for the wave-wave interaction terms to be large in the vorticity and thermodynamic equations, but to cancel in the potential vorticity equation, leaving a linear potential vorticity balance. Baroclinic calculations similar to the barotropic diagnoses described here are needed to address this possibility.

*Acknowledgments.* We thank S. Manabe, N.-C. Lau, and B. J. Hoskins for their helpful comments on this

work. In-Sik Kang was supported by NOAA and Princeton University under Grant NA 85-EAD00057.

#### REFERENCES

- Branstator, G., 1985a: Analysis of general circulation model sea-surface temperature anomaly simulations using a linear model. Part I: Forced solutions. *J. Atmos. Sci.*, **42**, 2225–2241.
- , 1985b: Analysis of general circulation model sea-surface temperature anomaly simulations using a linear model. Part II: Eigenanalysis. *J. Atmos. Sci.*, **42**, 2242–2254.
- Frederiksen, J. S., 1983: A unified three-dimensional instability theory of the onset of blocking and cyclogenesis. II: Teleconnection patterns. *J. Atmos. Sci.*, **40**, 2593–2609.
- Geisler, J. E., M. L. Blackmon, G. T. Bates and S. Munoz, 1985: Sensitivity of January climate response to the magnitude and position of equatorial Pacific sea surface temperature anomalies. *J. Atmos. Sci.*, **42**, 1037–1049.
- Held, I. M., R. L. Panetta and R. T. Pierrehumbert, 1985: Stationary external Rossby waves in vertical shear. *J. Atmos. Sci.*, **42**, 865–883.
- Hendon, H. H., 1986: The time-mean flow and variability in a nonlinear model of the atmosphere with tropical diabatic forcing. *J. Atmos. Sci.*, **43**, 72–88.
- Horel, J. D., and J. M. Wallace, 1981: Planetary-scale atmospheric phenomena associated with the Southern Oscillation. *Mon. Wea. Rev.*, **109**, 813–829.
- Hoskins, B. J., and D. J. Karoly, 1981: The steady linear response of a spherical atmosphere to thermal and orographic forcing. *J. Atmos. Sci.*, **38**, 1179–1196.
- Kang, I.-S., and I. M. Held, 1986: Linear and nonlinear diagnostic models of stationary eddies in the upper troposphere during Northern summer. *J. Atmos. Sci.*, **43**, 3045–3057.
- , and N.-C. Lau, 1986: Principle modes of atmospheric variability in model atmospheres with and without anomalous sea surface temperature forcing in the tropical Pacific. *J. Atmos. Sci.*, **43**, 2719–2735.
- Kok, C. J., and J. D. Opsteegh, 1985: On the possible causes of anomalies in seasonal mean circulation pattern during the 1982/83 El Niño event. *J. Atmos. Sci.*, **42**, 677–694.
- Lau, N.-C., 1985: Modeling the seasonal dependence of the atmospheric response to observed El Niños in 1962–76. *Mon. Wea. Rev.*, **113**, 1970–1996.
- Palmer, T. N., and D. A. Mansfield, 1986a: A study of wintertime circulation anomalies during past El Niño events, using a high resolution general circulation model. I: Influence of model climatology. *Quart. J. Roy. Meteor. Soc.*, **112**, 613–638.
- , and —, 1986b: A study of wintertime circulation anomalies during past El Niño events, using a high resolution general circulation model. II: Variability of the seasonal mean response. *Quart. J. Roy. Meteor. Soc.*, **112**, 639–660.
- Rasmusson, E., and T. Carpenter, 1982: Variations in tropical sea-surface temperature and surface wind fields associated with the Southern Oscillation/El Niño. *Mon. Wea. Rev.*, **110**, 354–384.
- Sardeshmukh, P. D., and B. J. Hoskins, 1985: Vorticity balances in the tropics during the 1982–1983 El-Niño Southern Oscillation event. *Quart. J. Roy. Meteor. Soc.*, **111**, 261–278.
- , and —, 1987: On the generation of global rotational flow by steady idealized tropical divergence. *J. Atmos. Sci.*, in press.
- Schneider, E. K., 1987: A formulation for diagnostic anomaly models. *Pure Appl. Geophys.*, in press.
- Simmons, A. J., J. M. Wallace and G. Branstator, 1983: Barotropic wave propagation and instability, and atmospheric teleconnection patterns. *J. Atmos. Sci.*, **40**, 1363–1392.